Quantum Frontiers
上海交通大學 SHANGHAI JIAO TONG UNIVERSITY 李政道研究所 Tsung-Dao Lee Institute

ORIGINAL ARTICLE Open Access

Quantum remote sensing with atom-light entangled interface

Minwei Shi[1], Sheng Ming[1], Shuhe Wu[1], Dong Zhang[1], Wei Du[1], Peiyu Yang[1], Guzhi Bao[1], Jinxian Guo[1*] and Weiping Zhang[1,2,3,4*]

Abstract

Quantum remote sensing utilizes quantum entanglement between the probe and the receiver to enhance the capability to sense a remote target. Quantum illumination is considered as a promising protocol to realize such a quantum technology in an environment of high loss and intense noise. However, the protocol requires an additional on-demand quantum memory, the imperfect performance of which diminishes the quantum advantage and limits the enhancement of sensing. In this paper, we propose a new protocol for quantum remote sensing based on quantum illumination with atom-light entangled interface. Compared to conventional light-only quantum illumination, the proposed protocol utilizes Raman coupling to create a long-lived atomic spin wave entangled with a Stokes light. The atomic spin wave, automatically built-in memory via the Raman coupling, acts as a local reference. The entangled Stokes light is used as a probe to irradiate a remote target. Meanwhile, the returned probe light from target is detected through coupling again to the atomic spin wave. A joint measurement on the returned probe light and spin wave is performed to discriminate the target. A 4 dB quantum enhancement over classical illumination is estimated. The atom-light entangled interface naturally integrates the quantum source, quantum memory, and quantum receiver in a single unit which exhibits great potential to develop highly compact and portable devices for quantum-enhanced remote sensing.

Keywords: Quantum remote sensing, Atom-light entangled interface, Raman process, Passive signature

1 Introduction

Remote sensing is to measure the target without physical contact, which can be applied in many fields, such as geography [1], land surveying [2], and Earth science [3]. To further improve performance, quantum remote sensing has been developed by utilizing quantum resources which attracts many attentions for decades [4–17]. However, inevitable losses and environmental noises diminish the nonclassicality of quantum resources which limit the application of most quantum remote sensing protocols in practical scenarios. As a promising protocol, quantum illumination (QI) is proposed which can maintain the quantum enhancement from entanglement under high levels of loss and noise [6–17].

Conventional optical QI uses a quantum entangled source to produce a pair of entangled probe and reference beams, in which the probe illuminates a remote target with low reflectivity embedded in a noisy environment, and the reference retains locally. When the probe returns, a joint measurement on the returned probe and reference beam is performed to estimate the quantum correlation between returned probe and reference so as to extract the information of target. In this process, two requirements of reference beam are essentially needed [11]: (1) the reference beam must be stored on demand to offset the time delay of probe during the detection round-trip; (2) the loss of reference beam should be avoided to protect the quantum correlation between returned probe and reference.

*Correspondence: jxguo@sjtu.edu.cn; wpz@sjtu.edu.cn
[1]School of Physics and Astronomy, and Tsung-Dao Lee Institute, Shanghai Jiao Tong University, Shanghai, 200240, China
[2]Shanghai Research Center for Quantum Sciences, Shanghai, 201315, China
Full list of author information is available at the end of the article

The first requirement can be achieved by storing the reference beam in a quantum memory like optical delay, atoms [18–21] and quantum dots [22, 23]. However, the loss of reference, dominantly induced by the imperfection of storage and retrieving operations [18–23], results in an additional damage of quantum correlation which goes against the second requirement.

Here we propose a more satisfactory protocol by directly entangling the light probe and on-demand quantum memory with atom-light entangled interface. As one of the widely-used atom-light entangled interface, Raman atom-light interaction has achieved many creative achievements, such as atom-light hybrid interferometer [24, 25] and high performance quantum memory [26]. In this paper, a remote sensing system is created based on Raman interaction in atomic ensemble which generates an entangled Stokes light and atomic spin wave. The Stokes field is used as a probe to illuminate the target. The atomic spin wave acts as an entangled reference, build-in quantum memory, and quantum receiver to perform joint measurement on the returned Stokes light. Two receiving strategies are developed in our atom-light remote sensing system which is known as phase conjugate (PC) and parametric amplification (PA) receiver. Compared with classical illumination, about 4 dB quantum enhancement can be achieved with PA receiver. Furthermore, the scheme integrates the quantum source, quantum memory and quantum receiver by using atom-light interaction which significantly prevents the quantum remote sensing system from the losses caused by the storage process of reference mode, offering great potential for reducing experiment flaws and showing larger quantum advantages experimentally.

This paper is organized as follows. In Sect. 2, we briefly introduce the basic protocol of QI with atom-light entangled interface. In Sect. 3, we introduce the atom-light entangled state based on Raman interaction. In Sect. 4, we model the quantum sensing process and give the atom-light state under each hypothesis. In Sect. 5, we design two quantum receivers based on linear and nonlinear atom-light interface, i.e. phase conjugate receiver and parametric amplification receiver. The performance of our protocol is also analyzed. Finally, it is summarized with discussion in Sect. 6.

2 Quantum illumination with atom-light entangled interface

Conventional optical quantum illumination protocol requires three basic elements: a quantum source, an on-demand quantum memory and a quantum receiver, as shown in Fig. 1(a). Firstly, a quantum source generates a pair of entangled probe and reference beam. Then, the probe is used to sense the target in the noisy environment, we can model the sensing process as a linear mixture of probe and thermal noise on a beam splitter which has reflectivity κ. The reference is directly stored in an on-demand quantum memory to wait for the joint measurement with returned probe. Finally, the reference is retrieved from the quantum memory when the probe returns from the target area. The quantum receiver performs a joint measurement on the retrieved reference and the returned probe to extract the information of the target. Theoretically, with proper entangled quantum source [7] and available receiver [9, 27], 3 dB quantum enhancement can be achieved compared to classical coherent illumination. Nevertheless, due to the loss of reference in the memory process and system nonidealities, only 0.8 dB quantum improvement is realized experimentally [11]. In order to fully exhibit the quantum advantage of quantum illumination, a more concise quantum remote sensing system is needed.

In our atom-light remote sensing system, the three basic elements of quantum illumination can be integrated into an atomic ensemble, as shown in Fig. 1(b). Firstly, a parametric amplification process such as Raman process [28, 29] and Faraday process [29, 30], is applied on the atomic ensemble to generate a probe light and an entangled atomic collective excitation. The atomic collective excitation, also known as atomic spin wave, has a long coherence time and can be retrieved into a light field on demand. The probe is sent to detect the target, the same as conventional optical QI, while the atomic spin wave is retained locally. When the atomic ensemble receives the returned probe, another atom-light interaction happens to interfere the probe with the spin wave. Then the output light field and spin wave generated by the interaction are measured to extract the quantum correlation, which can be used to infer the target's information. Therefore, the generation of entanglement, on-demand quantum memory, and receiving of the target's information are realized in a single atomic ensemble. This compact and highly integrated structure avoids the loss induced by reference storage and retrieving process, potentially realizing larger quantum advantage experimentally.

3 Atom-light entangled state

To establish a down-to-earth atom-light remote sensing system, we choose the Raman process in an ensemble of Λ-type atoms as the atom-light entangled interface. The energy levels of atoms are depicted in the inset of Fig. 1(b) which consist of a pair of metastable lower states ($|g\rangle$ and $|m\rangle$) and an excited state $|e\rangle$. The atoms are initially prepared in state $|g\rangle$ without population in $|m\rangle$ and $|e\rangle$, which corresponding to the vacuum state of spin wave operator $|0_A\rangle = |g\rangle^{\otimes N_a}$, where N_a is the number of atoms. To generate the atom-light entangled state, a strong coherent pump field couples the transition of atomic state $|g\rangle \leftrightarrow |e\rangle$ with large detuning Δ. Then the atoms in ground state $|g\rangle$ absorb the pump light and transit to the state $|m\rangle$ with the emission of Stokes field $\hat{a}_S$. Due to the two photon resonance condition of Raman process, the frequency of Stokes

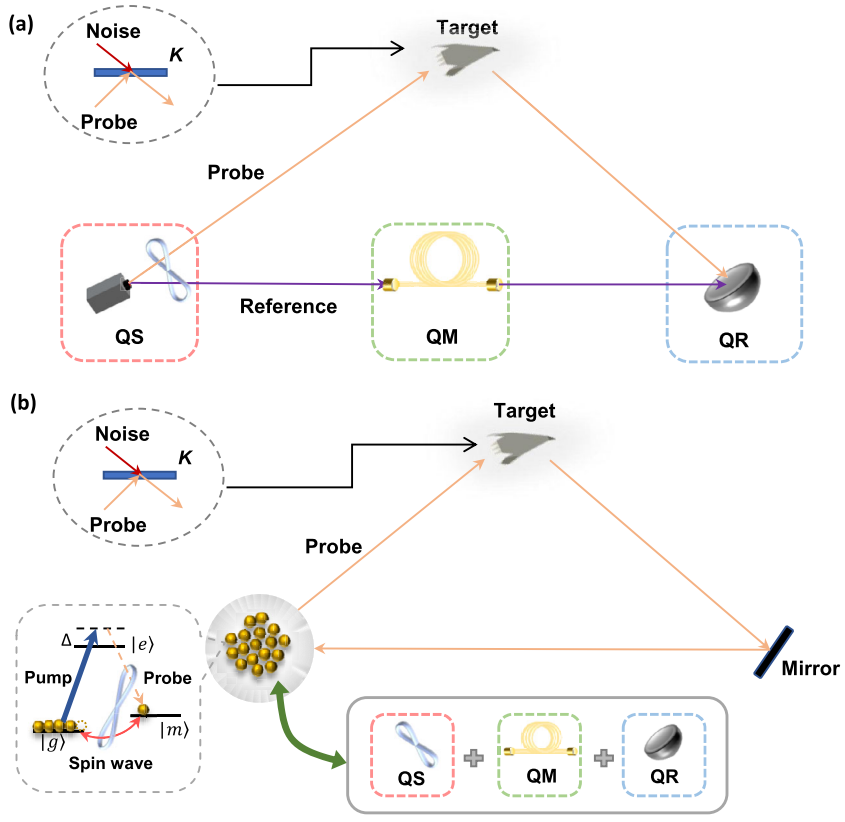

Figure 1 Schematics of (**a**) conventional quantum illumination which consists of three elements: quantum source, quantum memory and quantum receiver, and (**b**) atom-light quantum remote sensing system which integrates these three elements by atom-light entangled interface. The target can be modeled as a beam splitter with reflectivity of κ. Energy level in (**b**) shows one of the atom-light entangled interface based on Raman amplification process which generates the entanglement between probe and spin wave. QS: quantum source; QM: quantum memory; QR: quantum receiver

field $\omega_S = \omega_P - \omega_{mg}$, where ω_{mg} is the frequency difference between $|m\rangle$ and $|g\rangle$. Meanwhile, the transition of atoms from $|g\rangle \to |e\rangle \to |m\rangle$ generates a coherence between the two states which can be defined as a spin wave operator $\hat{S}_a = \frac{1}{\sqrt{N_a}} \sum_k^{N_a} |g\rangle_{kk}\langle m|$ (see Appendix A).

With the definition of spin wave, the Hamiltonian of Raman process in the interaction picture [28, 29] is

$$\hat{H} = i\hbar\eta A_P \hat{a}_S^\dagger \hat{S}_a^\dagger - i\hbar\eta A_P \hat{a}_S \hat{S}_a, \tag{1}$$

where $\eta = \sqrt{N_a} g^2/\Delta$ with the coupling coefficients g between the excited state and ground states. For simplicity but without loss of generality, we neglect the phase of pump field and set the pump field A_P real.

With vacuum input of Stokes field, the generated atom-light entangled state is

$$|\psi_{\rm AL}\rangle = \frac{1}{\cosh r} \sum_n \frac{(\hat{S}_a^\dagger \hat{a}_S^\dagger \tanh r)^n}{n!} |0\rangle_A |0\rangle_L, \tag{2}$$

where $r = |\eta A_P| t$ is the squeezing parameter, t is the atom-light interaction time. Therefore, the atom-light entangled state $|\psi_{\rm AL}\rangle$ is a two mode squeezed vacuum state, which belongs to the zero-mean Gaussian state. The corresponding density matrix $\hat{\rho}_{\rm AL} = |\psi_{\rm AL}\rangle\langle\psi_{\rm AL}|$ can be completely characterized by its covariance matrix $\Lambda_{\rm AL} = \langle [\hat{a}_S^\dagger \hat{a}_S \hat{S}_a^\dagger \hat{S}_a]^T [\hat{a}_S \hat{a}_S^\dagger \hat{S}_a \hat{S}_a^\dagger] \rangle$, which is

$$\Lambda_{\rm AL} = \begin{bmatrix} S & 0 & 0 & C \\ 0 & S & C & 0 \\ 0 & C & A & 0 \\ C & 0 & 0 & A \end{bmatrix}. \tag{3}$$

Here $S = \langle \hat{a}_S^\dagger \hat{a}_S \rangle = n_S$, $A = \langle \hat{S}_a^\dagger \hat{S}_a \rangle = n_S$ and $C = \langle \hat{a}_S \hat{S}_a \rangle = \langle \hat{a}_S^\dagger \hat{S}_a^\dagger \rangle = \sqrt{n_S(n_S+1)}$ where $n_S = \sinh^2 r$. Obviously, nonzero squeezing parameter $r > 0$ makes the entanglement metric $\varepsilon = |\langle \hat{S}_a \hat{a}_S \rangle| / \sqrt{\langle \hat{S}_a^\dagger \hat{S}_a \rangle \langle \hat{a}_S^\dagger \hat{a}_S \rangle} > 1$ which means that the Raman interaction can generate entanglement between Stokes light and atomic spin-wave.

4 Quantum sensing with atom-light interface

To detect the target, the generated Stokes light is emitted into the target area. While the atomic spin wave, whose quadrature fluctuation is highly correlated with the one of probe, can be durably maintained as a quantum memory. Under the hypothesis H_0 (target absence), we get a returned probe $\hat{a}_R = \hat{a}_B$ where $\hat{a}_B$ is the annihilation operator of the thermal field in environment with large average photon number $n_B = \langle \hat{a}_B^\dagger \hat{a}_B \rangle \gg 1$. Then the density matrix of retained atomic spin wave and the returned probe can be expressed by its covariance matrix

$$\Lambda_R^{(H_0)} = \begin{bmatrix} B & 0 & 0 & 0 \\ 0 & B & 0 & 0 \\ 0 & 0 & A & 0 \\ 0 & 0 & 0 & A \end{bmatrix}, \tag{4}$$

where $B = n_B$. Under the hypothesis H_1 (target presence), we can model the target as a beam splitter with reflectivity κ, as shown in Fig. 1. In this case, the returned probe consists of a weak probe reflected by the target and a large environmental noise field as $\hat{a}_R = \sqrt{\kappa}\hat{a}_S + \sqrt{1-\kappa}\hat{a}_B$. Considering the entire detection round-trip (including the loss of signal light during propagation and the reflectivity of the object), we set the total reflection coefficient $\kappa \ll 1$. Then the received atom-light state becomes

$$\Lambda_R^{(H_1)} = \begin{bmatrix} R & 0 & 0 & \sqrt{\kappa}C \\ 0 & R & \sqrt{\kappa}C & 0 \\ 0 & \sqrt{\kappa}C & A & 0 \\ \sqrt{\kappa}C & 0 & 0 & A \end{bmatrix}, \tag{5}$$

where $R = \langle \hat{a}_R^\dagger \hat{a}_R \rangle = \kappa n_S + (1-\kappa) n_B$ and $\sqrt{\kappa}C = \langle \hat{a}_R \hat{S}_a \rangle$. The diagonal term R contains the target information κ, representing the intensity change of returned probe caused by the target. The off-diagonal terms with $\sqrt{\kappa}$ in $\Lambda_R^{(H_1)}$ represent the residue quantum correlation between the spin wave and returned probe due to the entangled probe reflected by the target.

5 Atom-light interface as quantum receiver

To extract the target's information, a joint measurement is needed to estimate the covariance matrices. A receiver that perform interference between returned probe and the local spin wave can achieve the joint measurement. As we know, there are two types of interference in Raman atom-light interface: nonlinear interference based on Raman amplification process [24, 29, 31–34] and linear interference based on Rabi-like Raman oscillation [25, 33, 34]. Based on the two types of interference, the parametric amplification (PA) and phase conjugate (PC) receiver are designed.

5.1 Parametric amplification receiver

The PA strategy performs a Raman amplification process on the returned probe and atomic spin wave together (showing in Fig. 2) with the Hamiltonian

$$\hat{H}_{\mathrm{PA}} = i\hbar\eta A_P' \hat{a}_R \hat{S}_a - i\hbar\eta A_P' \hat{a}_R^\dagger \hat{S}_a^\dagger, \tag{6}$$

which can achieve nonlinear interference. The outputs of the nonlinear interference are

$$\hat{a}_S^{(d)} = \sqrt{G}\hat{a}_R - \sqrt{G-1}\hat{S}_a^\dagger, \tag{7}$$

$$\hat{S}_a^{(d)} = \sqrt{G}\hat{S}_a - \sqrt{G-1}\hat{a}_R^\dagger, \tag{8}$$

where the receiving gain $G = \cosh^2(|\eta A_P'|t')$ and t' is interaction time. Also, we ignore the phase of pump field and set A_P' real.

To obtain the target's information, the spin wave $\hat{S}^{(d)}$ is read out to perform intensity measurement [9] which gives the intensity of spin wave $N_1 = GA + (G-1)(R+1) - 2\sqrt{G(G-1)\kappa}C$ with variance $\sigma_1^2 = N_1(N_1+1)$ under hypothesis H_1 and $N_0 = GA + (G-1)(B+1)$ with variance $\sigma_0^2 = N_0(N_0+1)$ under hypothesis H_0.

We can discriminate between two hypotheses based on the measurement results. Due to the quantum fluctuation, the discrimination is not always correct. When these two hypotheses are equally likely, a Signal-to-Noise Ratio (SNR) $\mathrm{SNR} = (N_0 - N_1)^2/[2(\sigma_0 + \sigma_1)^2]$ [9, 27] is used to judge the validity of the discrimination. Higher SNR means lower error probability of discrimination and vice versa.

The SNR in our system using PA receiver is

$$\mathrm{SNR}_{\mathrm{PA}} = \frac{1}{2}\left[\frac{(G-1)\kappa(n_B - n_S)}{\sigma_0 + \sigma_1} + \frac{2\sqrt{G(G-1)\kappa n_S(n_S+1)}}{\sigma_0 + \sigma_1}\right]^2. \tag{9}$$

The first term in the binomial of $\mathrm{SNR}_{\mathrm{PA}}$ is the contribution of 'passive signature' while the second term represents the contribution from residue quantum correlation between returned probe and spin wave. Despite of the small change of noise when introducing 'passive signature', the SNR of our case is higher than the one reported in previous literature [9] due to the additional 'passive signature' term.

In order to further show the quantum advantage, the SNR of classical illumination (CI) [7] should also be discussed. Considering the effect of 'passive signature' [35], we can find that the optimal measurement strategy of CI is a combination of photon counting and homodyne measurement on the returned probe (see Appendix B). Due to the impossibility of simultaneously performing these two measurements, we always choose the measurement method with higher SNR, i.e. $\mathrm{SNR}_C = \max\{\mathrm{SNR}_{\mathrm{photon}}, \mathrm{SNR}_{\mathrm{homo}}\}$ as the performance of CI.

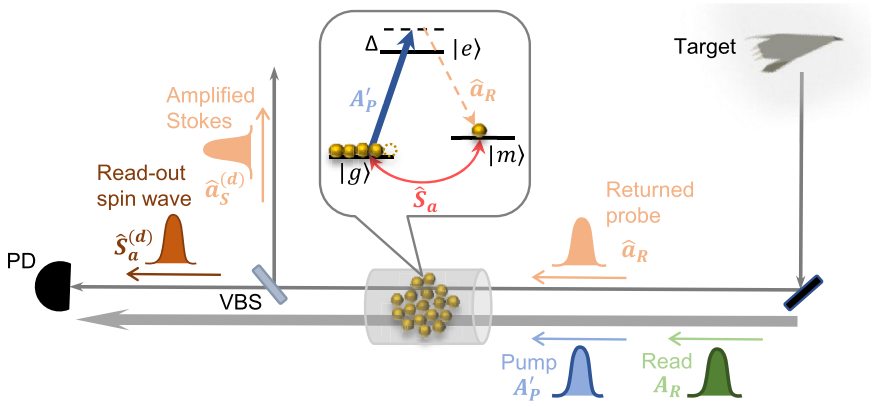

Figure 2 The illustration of PA receiving strategy. The returned probe (pink pulse, right) is sent into the atomic ensemble together with a pump field (blue pulse) to undergo a nonlinear interference with retained spin wave which generates an amplified Stokes field (pink pulse, left) and amplified spin wave. After the nonlinear interference process, the spin wave is read out into a light pulse (brown pulse) by a read light (green pulse). A variable beam splitter (VBS) is used to separate the amplified Stokes pulse (pink pulse, left) and the time-delayed read-out spin wave pulse (brown pulse). The splitting ratio of VBS can be temporally controlled. It reflects the amplified Stokes pulse when it arrives while the read-out spin wave can transmit through it later. Finally, The intensity measurement is performed on the read-out spin wave field (brown pulse). Inset: the energy level of the Raman amplification process. PD: photon detector

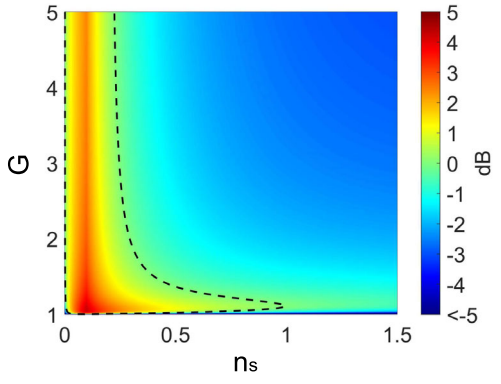

Figure 3 Quantum improvement $10\log_{10}(\mathrm{SNR_{PA}}/\mathrm{SNR_C})$ of atom-light sensing system with PA receiver versus the probe intensity n_S and receiving gain G. Here the total reflection coefficient $\kappa = 0.01$, the mean photon number of thermal noise $n_B = 20$. The region enclosed by dashed line with positive values is the quantum advantage regime

Then we can obtain the quantum enhancement through comparing the SNR of our protocol to the one of CI. The theoretical simulation shows that the quantum advantage of our system with PA receiver can reach about 4 dB compared to the optimal CI, as shown in Fig. 3. An additional 1 dB improvement of quantum enhancement is achieved by the passive signature in our system compared to the one mentioned in previous literature [9, 17].

Moreover, in the limit of $G \gg 1$, $\kappa \ll 1$, and $n_S \ll 1 \ll n_B$, we can eliminate G and $G-1$ from the numerator and the denominator of $\mathrm{SNR_{PA}}$ and simplify it to

$$\mathrm{SNR_{PA}} \approx \frac{1}{2}\left[\frac{\kappa}{2} + \frac{\sqrt{\kappa n_S}}{n_B}\right]^2. \tag{10}$$

The quantum advantage is larger than SNR_C as long as $n_S < \kappa n_B/2$. Correpsondingly, we can see that the quantum enhancement of our system can still be maintained when the receiving gain $G \gg 1$ in Fig. 3, unlike the previous work which requires a small gain $G - 1 \to 0$ [9].

5.2 Phase conjugate receiver

In PC type receiving strategy, the returned probe needs to undergo phase conjugation [9] before it interferes with the atomic spin wave. The phase conjugation can be realized by a non-degenerate four-wave mixing (FWM) process

$$\hat{a}_C = \sqrt{G}\hat{a}_V + \sqrt{G-1}\hat{a}_R^\dagger. \tag{11}$$

Here $\hat{a}_V$ represents the annihilation operator of the vacuum input of the idler port in the FWM process. The frequency of phase-conjugated returned probe $\hat{a}_C$ is Δ detuning to the transition $|g\rangle \leftrightarrow |e\rangle$ as shown in Fig. 4.

Then the phase-conjugated returned probe $\hat{a}_C$ is sent back to the atomic ensemble where the initial entanglement generates. Another pump field A''_P coupling the transition $|m\rangle \leftrightarrow |e\rangle$ with detuning Δ (as shown in Fig. 4) is sent to the ensemble for the linear interference of $\hat{a}_C$ and $\hat{S}_a$. The interaction is governed by the Hamiltonian

$$\hat{H}_{\mathrm{PC}} = i\hbar\eta A''_P \hat{a}_C^\dagger \hat{S}_a - i\hbar\eta^* A''^*_P \hat{a}_C \hat{S}_a^\dagger. \tag{12}$$

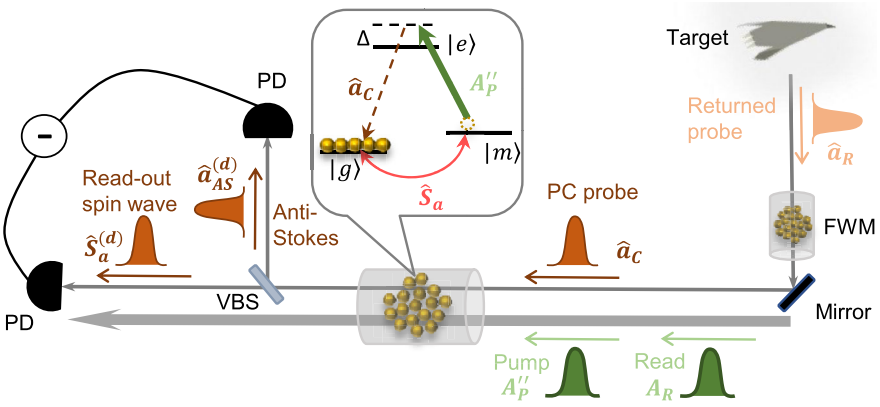

Figure 4 The illustration of PC receiving strategy. The returned probe (pink pulse) is phase conjugated by a four-wave-mixing process. Then the phase-conjugated probe (brown pulse, right) enters the atomic ensemble together with a pump field (green pulse, left) to undergo Rabi-like Raman interference. This interference generates an output Anti-Stokes field $\hat{a}_{AS}^{(d)}$ (brown pulse, middle) and an output spin wave $\hat{S}_a^{(d)}$ which is read out by the read light (green pulse, right) after the interference. The time-delayed read-out spin wave (brown pulse, left) is separated from the output Anti-Stokes (brown pulse, middle) by a variable beam splitter (VBS). The intensity measurement is performed on both output Anti-Stokes mode (brown pulse, middle) and read-out spin wave (brown pulse, left). Inset: the energy level of Rabi-like Raman oscillation process. PD: photon detector; PC probe: phase-conjugated probe

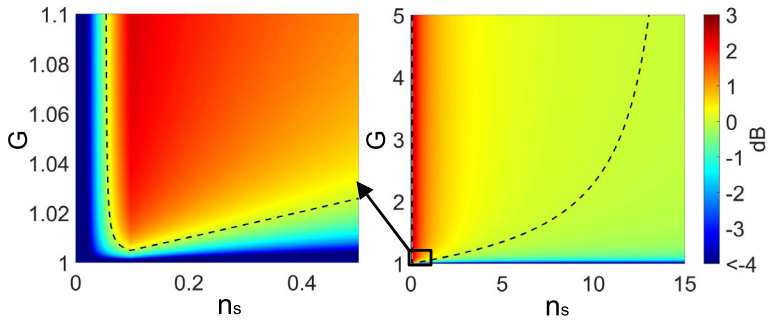

Figure 5 Quantum improvement $10\log_{10}(\mathrm{SNR_{PC}}/\mathrm{SNR_C})$ of atom-light sensing system with PC receiver versus the probe intensity n_S and receiving gain G. Here the total reflection coefficient $\kappa = 0.01$, the mean photon number of thermal noise $n_B = 20$. The area enclosed by dashed line with positive values is the quantum advantage regime

In order to extract the quantum correlation, the atom-light interaction should act as a 50-50 beam splitter which requires $|\eta A_p''|t'' = \pi/4$. The outputs of this atom-light beam splitter are

$$\hat{a}_{\mathrm{AS}}^{(d)} = (\hat{a}_C + \hat{S}_a)/\sqrt{2}, \tag{13}$$

$$\hat{S}_a^{(d)} = (\hat{a}_C - \hat{S}_a)/\sqrt{2}. \tag{14}$$

Then we read out the spin wave $\hat{S}_a^{(d)}$ after the linear receiving process and feed it into a unity-gain difference amplifier with $\hat{a}_{\mathrm{AS}}^{(d)}$, the equivalent joint measurement quantity is $\hat{N} = \hat{N}_X - \hat{N}_Y$ where $\hat{N}_X = \hat{a}_{\mathrm{AS}}^{(d)\dagger}\hat{a}_{\mathrm{AS}}^{(d)}$ and $\hat{N}_Y = \hat{S}_a^{(d)\dagger}\hat{S}_a^{(d)}$. The joint measurement gives that under hypothesis H_0 is $N_0 = 0$ with corresponding variance $\sigma_0^2 = (G-1)(2n_S n_B + n_S + n_B + 1) + Gn_S$ while $N_1 = 2\sqrt{(G-1)\kappa}C$ with variance $\sigma_1^2 = (G-1)[(1-\kappa)n_B(2n_S+1) + n_S(4\kappa n_S + 3\kappa + 1) + 1] + Gn_S$ under hypothesis H_1. The SNR is therefore given by

$$\mathrm{SNR_{PC}} = \frac{4(G-1)\kappa n_S(n_S+1)}{2(\sigma_0+\sigma_1)^2}, \tag{15}$$

As we can see, only the quantum correlation term are contained in the numerator of $\mathrm{SNR_{PC}}$ while the 'passive signature' κn_B only contribute to the variance. To further show the advantage, difference of SNR between the atom-light sensing system with PC receiver and CI are plotted in Fig. 5. In low probe intensity regime $n_S < 0.05$, the performance of our protocol by using PC receiver is inferior to the coherent sensor. This is because the signal $N_1 = 2\sqrt{(G-1)\kappa}C$ of our system only contains the contribution of quantum correlation which is near 0 for $n_S \to 0$. While

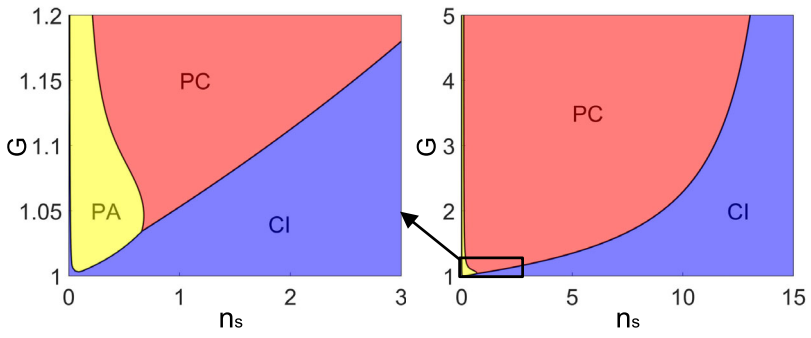

Figure 6 The region, where PA, PC or CI outperforms the others, is shown with various probe intensity n_S and receiving gain G. The total transmission coefficient $\kappa = 0.01$ and the mean photon number of thermal noise $n_B = 20$. Yellow region: PA receiver; Red region: PC receiver; Blue region: classical illumination

CI can still receive the target's information by just measuring the 'passive signature' even $n_S = 0$. With the increase of probe intensity n_S, the quantum correlation brings a significant increase in $\mathrm{SNR_{PC}}$, which quickly beats the one of CI and reaches 3 dB, the maximum quantum enhancement using PC receiver. Then, the quantum enhancement starts to decrease with the further increase of n_S, in accordance with previous works [7].

Further comparison between the performance of PA, PC, and CI for target detection are respectively shown in Fig. 6. we can see that the PC receiver (the red region in Fig. 6) achieves quantum advantage in a larger range of n_S, compared to the PA receiver (the yellow region). While PA receiver can only operate under a very low n_S regime to achieve a quantum improvement for target detection, see Fig. 6.

In addition, the area where our atom-light sensing system outperforms CI is figured out which gives two limits. When $G \gg 1$, $n_B \gg n_S$ and $\kappa \ll 1$, the maximum probe intensity to get the quantum advantage by PC receiver approaches $n_{S,\max} \approx (-1 + \sqrt{1 + 8\kappa n_B})/(4\kappa)$. When $n_S \ll 1$, the receiving gain should be larger than a critical number $G_{\mathrm{crit}} \approx 1 + n_S/n_B$ to get the quantum enhancement. With these two limitations, we can optimize our atom-light remote sensing system reasonably.

6 Conclusion and discussion

In conclusion, a remote sensing system is proposed based on the Raman atom-light entangled interface. In this system, the atom-light interface skillfully integrates the quantum source, quantum memory and quantum receiver together, making the quantum sensing system more concise and robust. Both parametric amplification receiver and phase conjugate receiver are realized in this protocol with 4 dB quantum enhancement in target detection by considering the 'passive signature'. Such an integrated structure significantly prevents the losses caused by the storage process of reference mode, offering great potential for robust and high performance remote quantum sensing.

In this system, the decay of atomic spin wave may restrict the distance between quantum source and target. For Raman process with geometrically wide optical modes, the decoherence of spin wave in ^{87}Rb atomic ensemble at $\sim 75°\mathrm{C}$ is mainly due to the atom-atom and atom-wall collisions caused by the thermal motion. The atom-atom collision induces a spin exchange relaxations rate $\gamma_{\mathrm{SE}} = 565.7\,\mathrm{s}^{-1}$ and the atom-wall collision induces a spin destruction relaxations rate $\gamma_{\mathrm{SD}} = 0.2828\,\mathrm{s}^{-1}$, resulting in a maximum memory time $T \approx 1.22\,\mathrm{ms}$ which guarantees the quantum advantage. This enables the atom-light remote sensing system to detect the target at nearly 183.7 km away. A longer distance can be realized by using cells with inert buffer gases and/or paraffin-coated cells which further extend the coherence time. Furthermore, non-dominant spin wave decoherence due to magnetic fields can be effectively eliminated by placing the cell in a magnetic shield. When all these effects are restrained, the coherence time can reach $\sim 60\,\mathrm{s}$ [36].

Appendix A: Definition of pseudo-spin wave operator $\hat{S}_a$

By adiabatically elimiate the excited state $|e\rangle$ under Raman condition, the remaining two ground states ($|g\rangle$ and $|m\rangle$) can be conveniently represented by angular momentum operators

$$\hat{J}_+ = \hat{J}_x + i\hat{J}_y = \sum_k^{N_a} |g\rangle_{kk}\langle m|, \tag{A.1}$$

$$\hat{J}_- = \hat{J}_x - i\hat{J}_y = \sum_k^{N_a} |m\rangle_{kk}\langle g|, \tag{A.2}$$

$$\hat{J}_z = \frac{1}{2}\sum_k^{N_a}\left(|g\rangle_{kk}\langle g| - |m\rangle_{kk}\langle m|\right), \tag{A.3}$$

where k represents the k-th atom. The above angular momentum operators obey the commutation relation $[J_+, J_-] = 2J_z$. Under the limit of low excitation ($\langle \hat{J}_-\hat{J}_+\rangle \ll N_a$) and large number of atoms($N_a \gg 1$), we can replace the $\hat{J}_z$ operator with its expectation value $\langle \hat{J}_z\rangle \approx N_a/2$. For simplicity, a new pair of atomic collective creation and annihilation operators [37, 38] can be defined as

$$\hat{S}_a = \frac{\hat{J}_+}{\sqrt{2\langle \hat{J}_z\rangle}} \approx \frac{1}{\sqrt{N_a}}\sum_k^{N_a}|g\rangle_{kk}\langle m|, \tag{A.4}$$

$$\hat{S}_a^\dagger = \frac{\hat{J}_-}{\sqrt{2\langle \hat{J}_z\rangle}} \approx \frac{1}{\sqrt{N_a}}\sum_k^{N_a}|m\rangle_{kk}\langle g||. \tag{A.5}$$

The above pseudo-spin wave operator $\hat{S}_a$ obeys the quasi-bosonic canonical commutation relation $[\hat{S}_a, \hat{S}_a^\dagger] \simeq 1$, which is consistent with the conclusion of Holstein–Primakoff transformation [39] in weak interation limit.

Appendix B: The optimal measurement strategy of classical illumination

For classical illumination, the probe is the coherent state $\hat{\rho} = |\alpha\rangle\langle\alpha|$. The returned probe state from the target area is then given by

$$\begin{aligned}\hat{\rho}_r &= \mathrm{Tr}_B\left[\hat{U}_\kappa\hat{\rho}\otimes\hat{\rho}_B\hat{U}_\kappa^\dagger\right]\\ &= \mathrm{Tr}_B\left[\hat{U}_\kappa\hat{D}(\alpha)\hat{U}_\kappa^\dagger\cdot\hat{U}_\kappa|0\rangle\langle 0|\otimes\hat{\rho}_B\hat{U}_\kappa^\dagger\right.\\ &\quad\left.\times\hat{U}_\kappa\hat{D}^\dagger(\alpha)\hat{U}_\eta^\kappa\right],\end{aligned} \tag{B.1}$$

where $\hat{\rho}_B$ is the density matrix of the thermal noise and $\hat{U}_\kappa$ is the evolution operator of signal-noise interaction modeled as a beam splitter. The first and third term in above equation can be expressed as two displacement operators that acting on the signal and thermal channel, respectively. i.e. $\hat{U}_\kappa\hat{D}(\alpha)\hat{U}_\kappa^\dagger = \hat{D}_S(\sqrt{\kappa}\alpha)\hat{D}_B(\sqrt{1-\kappa}\alpha)$. The middle term describes the linear mixing of vacuum state and the thermal noise, which gives two modified thermal states in each channel $\hat{U}_\kappa|0\rangle\langle 0|\otimes\hat{\rho}_B\hat{U}_\kappa^\dagger = \hat{\rho}_{B'}\otimes\hat{\rho}_{B''}$. After tracing over the thermal noise mode, one can conclude that the returned probe of CI is in a displaced thermal state

$$\hat{\rho}_r = \hat{D}_S(\sqrt{\kappa}\alpha)\hat{\rho}_{B'}\hat{D}_S^\dagger(\sqrt{\kappa}\alpha), \tag{B.2}$$

where $\hat{\rho}_{B'} = \sum_n^\infty \frac{n_{B'}^n}{(1+n_{B'})^{1+n}}|n\rangle\langle n|$ is the modified thermal state with mean photon number $n_{B'} = (1-\kappa)n_B$. $\hat{\rho}_r$ can be reorganized into diagonalized form

$$\hat{\rho}_r = \sum_n^\infty T_n|\psi_n\rangle\langle\psi_n|, \tag{B.3}$$

where $T_n = (1-\kappa)^n n_B^n/[1+(1-\kappa)n_B]^{1+n}$ and $|\psi_n\rangle = \hat{D}_S(\sqrt{\kappa}\alpha)|n\rangle$ is the diplaced Fock state with $\langle\psi_{n'}|\psi_n\rangle = \delta_{n',n}$.

The quantum Fisher information can then be given by

$$\begin{aligned}F_\kappa &= \sum_n^\infty\frac{\partial_\kappa T_n\cdot\partial_\kappa T_n}{T_n} + 4\sum_n^\infty T_n\,\mathrm{Re}\left(\langle\partial_\kappa\psi_n|\partial_\kappa\psi_n\rangle\right)\\ &\quad - 8\sum_{n,m}^\infty\frac{T_nT_m}{T_n+T_m}\mathrm{Re}\big(\langle\partial_\kappa\psi_m|\psi_n\rangle\\ &\quad\times\langle\psi_n|\partial_\kappa\psi_m\rangle\big).\end{aligned} \tag{B.4}$$

Some relevant inner products can be evaluated

$$\langle\psi_n|\partial_\kappa\psi_n\rangle = 0, \tag{B.5a}$$

$$\langle\psi_{n-1}|\partial_\kappa\psi_n\rangle = -\frac{1}{2}\sqrt{\frac{n}{\kappa}}\alpha, \tag{B.5b}$$

$$\langle\psi_n|\partial_\kappa\psi_{n-1}\rangle = \frac{1}{2}\sqrt{\frac{n}{\kappa}}\alpha, \tag{B.5c}$$

$$\langle\partial_\kappa\psi_n|\partial_\kappa\psi_n\rangle = \frac{\alpha^2}{4\kappa}(2n+1) \tag{B.5d}$$

and the derivative of T_n is

$$\partial_\kappa T_n = T_n\frac{(1-\kappa)n_B - n}{(1-\kappa)[1+(1-\kappa)n_B]} \tag{B.6}$$

Substituting Eq. (B.5a)–(B.5d) and Eq. (B.6) into Eq. (B.4), we obtain the quantum Fisher information

$$F_\kappa = \frac{n_B}{(1-\kappa)[1+(1-\kappa)n_B]} + \frac{\alpha^2}{\kappa[1+2(1-\kappa)n_B]} \tag{B.7}$$

For quantum single-parameter estimation, the optimal estimating precision is bounded by quantum Cramer–Rao bound. The eigenbasis of the symmetric logarithmic derivative (SLD) indicates the optimal measurement strategy that saturates the Cramer–Rao bound. The SLD is given by

$$\begin{aligned}\hat{L}_\kappa &= \sum_n^\infty\frac{\partial_\kappa T_n}{T_n}|\psi_n\rangle\langle\psi_n|\\ &\quad + 2\sum_{n,m}^\infty\frac{T_n - T_m}{T_n+T_m}\langle\psi_m|\partial_\kappa\psi_n\rangle|\psi_m\rangle\langle\psi_n|.\end{aligned} \tag{B.8}$$

The optimal observable is $\hat{O}_\kappa = \hat{L}_\kappa/F_\kappa$. Substituting Eq. (B.5a)–(B.5d) and (B.6) into Eq. (B.8), we have $\hat{O}_\kappa \propto k_1\hat{a}^\dagger\hat{a} + k_2(\hat{a}^\dagger + \hat{a})$, where k_1 and k_2 are coefficients. Therefore, the optimal measurement stragety for estimating κ is a combination of photon counting and homodyne measurement.

Acknowledgements
We acknowledge financial support from the Innovation Program for Quantum Science and Technology 2021ZD0303200, the National Science Foundation of China (Grant NO. 12234014, 11904227, 12204304, 11654005), Shanghai Municipal Science and Technology Major Project (Grant NO. 2019SHZDZX01), the Sailing Program of Shanghai Science and Technology Committee under Grant 19YF1421800, the Fundamental Research Funds for the Central Universities, and the Fellowship of China Postdoctoral Science Foundation (Grant No. 2020TQ0193, 2021M702146, 2021M702150, 2021M702147, 2022T150413), and the National Key Research and Development Program of China under Grant number 2016YFA0302001. W.Z. also acknowledges additional support from the Shanghai talent program.

Funding
Open access funding provided by Shanghai Jiao Tong University.

Availability of data and materials
The data and materials that support the findings of this study are available from the corresponding author upon reasonable request.

Declarations

Competing interests
All authors declare that there are no competing interests.

Author contribution
MS performed theory, and simulations under the supervision of JG and WZ. MS, JG, GB, and WZ wrote the manuscript. All authors contributed to the discussions and approved the final manuscript. The project is supervised by WZ.

Author details
[1]School of Physics and Astronomy, and Tsung-Dao Lee Institute, Shanghai Jiao Tong University, Shanghai, 200240, China. [2]Shanghai Research Center for Quantum Sciences, Shanghai, 201315, China. [3]Collaborative Innovation Center of Extreme Optics, Shanxi University, Taiyuan, 030006, China. [4]Shanghai Branch, Hefei National Laboratory, Shanghai, 201315, China.

Publisher's Note

Received: 7 November 2022 Revised: 7 November 2022
Accepted: 16 November 2022 Published online: 01 December 2022

References

1. Curran PJ (1987) Review article remote sensing methodologies and geography. Int J Remote Sens 8:1255–1275
2. Gallego FJ (2004) Remote sensing and land cover area estimation. Int J Remote Sens 25:3019–3047
3. Hugenholtz CH, Moorman BJ, Riddell K, Whitehead K (2012) Small unmanned aircraft systems for remote sensing and Earth science research. Eos Trans AGU 93:236
4. Zhang W, Zhang D, Qiu X, Chen L (2019) Quantum remote sensing of the angular rotation of structured objects. Phys Rev A 100:043832
5. Okane H, Hakoshima H, Takeuchi Y, Seki Y, Matsuzaki Y (2021) Quantum remote sensing under the effect of dephasing. Phys Rev A 104:062610
6. Lloyd S (2008) Enhanced sensitivity of photodetection via quantum illumination. Science 321:1463–1465
7. Tan SH, Erkmen BI, Giovannetti V, Guha S, Lloyd S, Maccone L, Pirandola S, Shapiro JH (2008) Quantum illumination with Gaussian states. Phys Rev Lett 101:253601
8. Zhuang Q, Zhang Z, Shapiro JH (2017) Optimum mixed-state discrimination for noisy entanglement-enhanced sensing. Phys Rev Lett 118:040801
9. Guha S, Erkmen BI (2009) Gaussian-state quantum-illumination receivers for target detection. Phys Rev A 80:052310
10. Lopaeva ED, Berchera IR, Degiovanni IP, Olivares S, Brida G, Genovese M (2013) Experimental realization of quantum illumination. Phys Rev Lett 110:153603
11. Zhang Z, Mouradian S, Wong FN, Shapiro JH (2015) Entanglement-enhanced sensing in a lossy and noisy environment. Phys Rev Lett 114:110506
12. Barzanjeh S, Pirandola S, Vitali D, Fink JM (2020) Microwave quantum illumination using a digital receiver. Sci Adv 6:eabb0451
13. Nair R, Gu M (2020) Fundamental limits of quantum illumination. Optica 7:771–774
14. Calsamiglia J, De Vicente JI, Muñoz-Tapia R, Bagan E (2010) Local discrimination of mixed states. Phys Rev Lett 105:080504
15. England DG, Balaji B, Sussman BJ (2019) Quantum-enhanced standoff detection using correlated photon pairs. Phys Rev A 99:023828
16. Chang CS, Vadiraj AM, Bourassa J, Balaji B, Wilson CM (2019) Quantum-enhanced noise radar. Appl Phys Lett 114:112601
17. Sanz M, Las Heras U, García-Ripoll JJ, Solano E, Di Candia R (2017) Quantum estimation methods for quantum illumination. Phys Rev Lett 118:070803
18. Specht HP, Nölleke C, Reiserer A, Uphoff M, Figueroa E, Ritter S, Rempe G (2011) A single-atom quantum memory. Nature 473:190–193
19. Lvovsky AI, Sanders BC, Tittel W (2009) Optical quantum memory. Nat Photonics 3:706–714
20. Kozhekin AE, Mølmer K, Polzik E (2000) Quantum memory for light. Phys Rev A 62:033809
21. Vernaz-Gris P, Huang K, Cao M, Sheremet AS, Laurat J (2018) Highly-efficient quantum memory for polarization qubits in a spatially-multiplexed cold atomic ensemble. Nat Commun 9:1–6
22. Tang JS, Zhou ZQ, Wang YT, Li YL, Liu X, Hua YL et al (2015) Storage of multiple single-photon pulses emitted from a quantum dot in a solid-state quantum memory. Nat Commun 6:1–7
23. Wolters J, Buser G, Horsley A, Béguin L, Jöckel A, Jahn JP et al (2017) Simple atomic quantum memory suitable for semiconductor quantum dot single photons. Phys Rev Lett 119:060502
24. Chen B, Qiu C, Chen S, Guo J, Chen LQ, Ou ZY, Zhang W (2015) Atom-light hybrid interferometer. Phys Rev Lett 115:043602
25. Qiu C, Chen S, Chen LQ, Chen B, Guo J, Ou ZY, Zhang W (2016) Atom-light superposition oscillation and Ramsey-like atom-light interferometer. Optica 3:775–780
26. Guo J, Feng X, Yang P, Yu Z, Chen L, Yuan C, Zhang W (2019) High-performance Raman quantum memory with optimal control in room temperature atoms. Nat Commun 10:1–6
27. Jo Y, Lee S, Ihn YS, Kim Z, Lee SY (2021) Quantum illumination receiver using double homodyne detection. Phys Rev Res 3:013006
28. Duan LM, Lukin MD, Cirac JI, Zoller P (2001) Long-distance quantum communication with atomic ensembles and linear optics. Nature 414:413–418
29. Hammerer K, Sørensen AS, Polzik ES (2010) Quantum interface between light and atomic ensembles. Rev Mod Phys 82:1041
30. Madsen LB, Mølmer K (2004) Spin squeezing and precision probing with light and samples of atoms in the Gaussian description. Phys Rev A 70:052324
31. Ma H, Li D, Yuan CH, Chen LQ, Ou ZY, Zhang W (2015) SU (1, 1)-type light-atom-correlated interferometer. Phys Rev A 92:023847
32. Raymer MG, Mostowski J (1981) Stimulated Raman scattering: unified treatment of spontaneous initiation and spatial propagation. Phys Rev A 24:1980
33. Chen LQ, Zhang GW, Bian CL, Yuan CH, Ou ZY, Zhang W (2010) Observation of the Rabi oscillation of light driven by an atomic spin wave. Phys Rev Lett 105:133603
34. Chen LQ, Bian CL, Zhang GW, Ou ZY, Zhang W (2010) Observation of temporal beating in first-and second-order intensity measurement between independent Raman Stokes fields in atomic vapor. Phys Rev A 82:033832
35. Pirandola S, Bardhan BR, Gehring T, Weedbrook C, Lloyd S (2018) Advances in photonic quantum sensing. Nat Photonics 12:724–733
36. Balabas MV, Karaulanov T, Ledbetter MP, Budker D (2010) Polarized alkali-metal vapor with minute-long transverse spin-relaxation time. Phys Rev Lett 105:070801
37. Julsgaard B, Kozhekin A, Polzik ES (2001) Experimental long-lived entanglement of two macroscopic objects. Nature 413:400–403
38. Sherson JF, Krauter H, Olsson RK, Julsgaard B, Hammerer K, Cirac I, Polzik ES (2006) Quantum teleportation between light and matter. Nature 443:557–560
39. Holstein T, Primakoff H (1940) Field dependence of the intrinsic domain magnetization of a ferromagnet. Phys Rev 58:1098